

Supporting Information

Quantum yields of singlet and triplet chemiexcitation of dimethyl

1,2-Dioxetane: Ab initio nonadiabatic molecular dynamics simulation

Ling Yue,^{ab} Le Yu,^c Chao Xu,^d Chaoyuan Zhu^{*ade} and Yajun Liu^{*f}

1 Global Switching Probability for Conical Intersection and Intersystem Crossing.....	2
Figure S1. The diabatic and adiabatic PESs at the crossing region.....	2
Figure S2. The three cases of nonadiabatic transition.....	3
2 Initial Sampling with One-Dimension Square Barrier Potential Approximation.....	4
Figure S3. The one-dimensional rectangular barrier potential.	4
Figure S4. The distribution of the velocities, the number of positive (N^+) and negative (N^-) trajectories and the N^+/N^- before and after resampling with 10000 trajectories.	6
Figure S5. The distribution of the velocities, the number of positive (N^+) and negative (N^-) trajectories and the N^+/N^- before and after resampling with 300 trajectories	6
3 Implementation of Global Switching Algorithm in Newton-X.....	6
Figure S6. Flowchart of global switching algorithm implemented in Newton-X package.	8
4 The Other Figures and Tables.....	9
Figure S7. The active orbitals of 8-in-6 active space used in SA-CASSCF computation.....	9
Figure S8. The labels of atoms and the scheme of the mixing basis sets.....	9
Table S1. The serial number of the internal coordinates.....	10
Figure S9. The comparison of the optimized bond lengths, bond angles and dihedral angles between the mixing and ANO-RCC-VDZP basis sets at SA-CASSCF(8,6) level.	11
Figure S10. The comparison of the optimized bond lengths, bond angles and dihedral angles between the mixing and ANO-RCC-VDZP basis sets at SA-CASSCF(8,6) level	11
Table S2. The key geometric parameters optimized by SA-CASSCF (normal) and CASPT2 (bold) method with 6-31G [*] +STO-3G mixed basis set (negative paths).	12
Figure S11. Time evolution of the ensemble-averaged bond lengths of O ₁ –O ₂ and C ₃ –C ₄ with standard deviations.....	13
Figure S12. Time evolution of the potential energies and key geometries of a typical trajectory which ends on the ground S ₀ state.	13
Figure S13. Time evolution of the potential energies and key geometries of a typical trajectory which ends on the excited S ₁ state.	14
Figure S14. Time evolution of the potential energies and key geometries of a typical trajectory which ends on the excited T ₁ state.	14
5 The Optimized Cartesian Coordinates (Å) at SA-CASSCF and CASPT2 Levels.....	15
6. Detailed internal geometries.....	26
7. Spin-orbital coupling matrix elements.....	28
References	32

1. Global Switching Probability for Conical Intersection and Intersystem Crossing.

The global switching algorithm makes trajectory hopping at the time t where $d(t) = |U_2(t) - U_1(t)|/|V_2(t) - V_1(t)|$ reaches local maximum, where the U_2 and U_1 are two adjacent adiabatic PESs, while the V_2 and V_1 are the corresponding two spin-pure diabatic potential energy surfaces as shown in Figure S1.

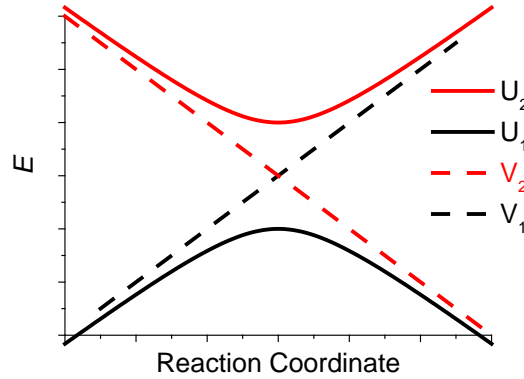


Fig. S1 The diabatic and adiabatic PESs at the crossing region.

In general, the analytical switching probability can be expressed in terms of $d(t)$ as:¹

$$\frac{\sinh[\delta(d^2-1)]}{\sinh(d^2\delta)} e^{-\delta} \xrightarrow{d \gg 1} e^{-2\delta},$$

in which δ is estimated from two potential energy surfaces (PESs) and the corresponding gradients at hopping point along on-the-fly running trajectory and δ is evaluated by^{2,3}

$$\delta = -\frac{\pi}{8\sqrt{a^2}} \sqrt{\frac{2}{b^2 + \sqrt{|b^4 \pm 1|}}}.$$

In the case of conical intersection (between the same spin multiplicity states) and intersystem crossing (between different spin multiplicity states), the nonadiabatic switching probability p is evaluated from

$$p = \begin{cases} e^{-2\delta} & \text{between states with same spin multiplicity (Figure S2A)} \\ 1 - e^{-2\delta} & \text{between states with different spin multiplicity (Figure S2B)} \end{cases}$$

In the other cases ($d \approx 1$), the nonadiabatic probability between two spin-pure PES with different spin (Figure S2C) is calculated by:

$$p = 1 - \frac{e^{-2\delta}}{e^{-2\delta} + 1}$$

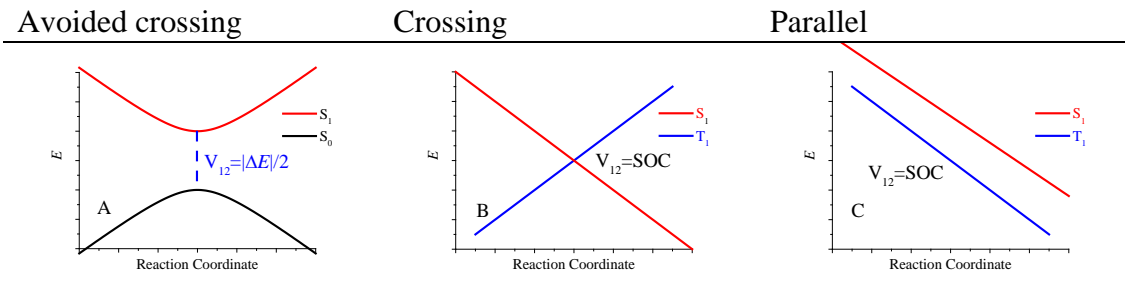


Fig. S2 The three cases of the nonadiabatic transition.

The two parameters, effective coupling parameter a^2 and effective collision energy b^2 are given by,

$$a^2 = \frac{\hbar^2 \sqrt{|F_2 F_1|} |F_2 - F_1|}{2\mu (2V_{12})^3},$$

and

$$b^2 = (E_t - E_x) \frac{|F_2 - F_1|}{\sqrt{|F_2 F_1|} (2V_{12})}.$$

In the present implementation along the on-the-fly trajectory, the global switching probability between same spin multiplicity states (Figure S2A), the diabatic forces F_j and F_i are generalized from the spin-pure adiabatic forces of three consecutive time steps by a simple diabatization procedure,⁴ and the half of the minimum energy gap ($|\Delta E|/2$) between two PESs (e.g. S_0/S_1 or T_1/T_2) at the avoided crossing region is approximately considered as diabatic coupling V_{12} . The detail procedures for multi-dimensional generalization along the on-the-fly trajectory is given in Ref. 4. For the global switching probability between different spin multiplicity states (Figure S2B) or parallel case (Figure S2C), the spin-diabatic representation is directly used, so that the diabatic forces F_j and F_i are directly computed by the gradients of the spin-pure states, and the diabatic coupling V_{12} is the effective spin-orbit coupling strengths (SOC) between the spin-pure states (e.g. S_0/T_1).^{5,6} The effective SOCs⁵ are approximated as the total length of the spin-orbit coupling vector **SOC**. For example, the SOC between a singlet i and a triplet state j is calculated by:

$$SOC_{ij} = \sqrt{\sum_{m=0,\pm 1} |\langle S_{m_s=0}^i | H_{SO} | T_{m_s=m}^j \rangle|^2}$$

where the SOC matrix elements are calculated at the *ab initio* complete active space self-consistent field (CASSCF) level.

If the spin-orbit interaction has small changes along with the variation of geometries (e.g. the excited-state intramolecular proton transfer process of o-nitrophenol),⁶ the SOC values between the interested states can be approximately set to be constant which is computed beforehand. Alternatively, the SOC can be also calculated on-the-fly during the GS-TSH simulation.

2. Initial Sampling with One-Dimension Square Barrier Potential Approximation.

At the ground-state minimum in equilibrium where the eigenvalues of the hessian matrix are all positive. The distribution of the initial geometric coordinates and velocities (momentums) could be obtained by the Boltzmann random sampling or Wigner sampling. However, along the reaction path there is the transition state where vibrational frequency is imaginary. Initial condition along this reaction path at the transition state is quantum flux ratio that is ratio between numbers of trajectories forward and backward to product (the other normal modes with positive vibrational frequencies can be still described by the Boltzmann or Wigner distribution in initial condition set up). We try to obtain this ratio by employing one-dimensional square barrier potential as shown in Figure S3.

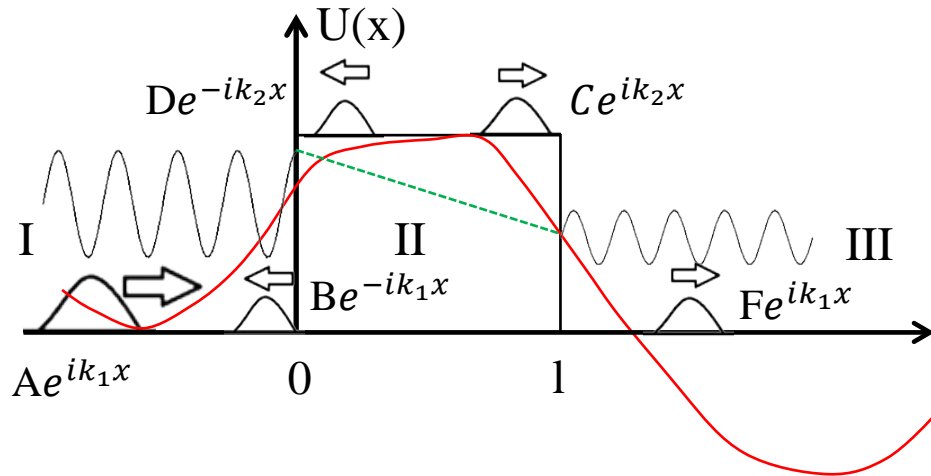


Fig. S3 The one-dimensional rectangular barrier potential.

Then, the time-independent Schrödinger equation can be written as:

$$-\frac{\hbar^2}{2m} \frac{\partial^2}{\partial x^2} \psi(x) = E\psi(x), x < 0 \text{ or } x > l$$

and

$$-\frac{\hbar^2}{2m} \frac{\partial^2}{\partial x^2} \psi(x) + V\psi(x) = E\psi(x), 0 \leq x \leq l$$

where the height of the box V represents the activation energy of the transition state. The general solution of the equation can be easily obtained as

$$\psi_I(x) = A \cdot e^{ik_1 x} + B \cdot e^{-ik_1 x},$$

$$\psi_{II}(x) = C \cdot e^{ik_2 x} + D \cdot e^{-ik_2 x},$$

and

$$\psi_{III}(x) = F \cdot e^{ik_1 x} + G \cdot e^{-ik_1 x}$$

where $k_1 = \frac{\sqrt{2mE}}{\hbar}$ and $k_2 = \frac{\sqrt{2m(E-V)}}{\hbar}$. The parameters A~G are constants which represent flux amplitudes of scattering waves. Suppose a wave pack transmits from the left to right side through the one-dimension square barrier potential. Due to the energetic barrier, both the incident wave ($A \cdot e^{ik_1 x}$) and reflected wave ($B \cdot e^{-ik_1 x}$) exist in region I (reactant), and only transmission wave exists in region III (product), i.e. $G=0$. Using the boundary condition $\psi_I(0) = \psi_{II}(0)$ and $\psi_{II}(l) = \psi_{III}(l)$, the ratio between the wave ($C \cdot e^{ik_2 x}$) forward to product and the wave ($D \cdot e^{-ik_2 x}$) backward to product (at transition state) can be obtained in the case of $E > V$ as

$$\left| \frac{C}{D} \right|^2 = \left(\frac{k_1 + k_2}{k_1 - k_2} \right)^2 = \left(\frac{\sqrt{E} + \sqrt{E-V}}{\sqrt{E} - \sqrt{E-V}} \right)^2$$

This quantum flux ratio is what we need for initial sampling trajectories at transition state. The initial velocities along the direction of reaction path is firstly sampled by Boltzmann distribution, the directions of these initial velocities (i.e. plus-minus sign) are adjusted by ensuring this ratio

$$\frac{N_+}{N_-} = \left| \frac{C}{D} \right|^2$$

where N_+ (N_-) is the number of trajectories forward (backward) to product whose velocities along the direction of reaction path are positive (negative). This ratio at TS is now implemented in modified Newton-X program.

For example, the initial velocity of an ensemble with 10000 trajectories is firstly obtained by Boltzmann sampling as initial starting kinetic energy 4.04 eV. The number of N_+ and N_- , the N_+/N_- together with the $|C/D|^2$ are plotted in Figure S4 as distributions of the velocity along the direction of the reaction path. It is obvious that the number of positive (N_+) and negative (N_-) trajectories are nearly the same with each other, the distribution of the velocity is almost symmetric, while the velocities are resampled, the center of the velocity distribution moves rightward slightly, and the number of positive trajectories (N_+) is obviously more than the negative one (N_-). The N_+/N_- fits the theoretical values of the $|C/D|^2$ quite well especially at the high-energy region.

Another set of ensemble with 300 trajectories is also resampled with initial starting kinetic energy 4.04 eV. The number of positive (N^+) and negative (N^-) trajectories, the N^+/N^- and the theoretical $|C/D|^2$ along the kinetic energy after resampling are plotted in Figure S5. Though the number of trajectories is , the N_+/N_- still fits the theoretical values of the $|C/D|^2$ well. This ensemble is used to be simulated in the text.

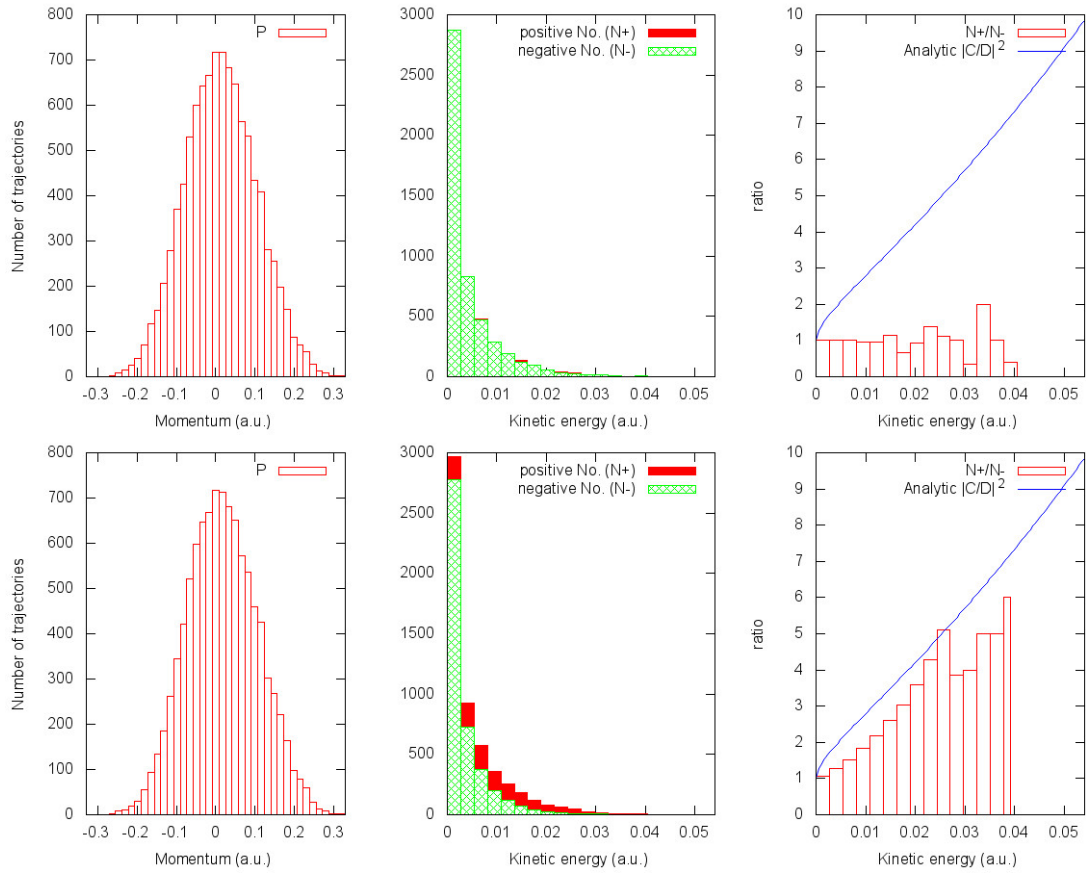


Fig. S4 The upper (lower) panel stands for the distribution of the velocities, the number of positive (N^+) and negative (N^-) trajectories, the ratio $N_+/N_- = |C/D|^2$, respectively along the direction of the reaction path according to the original Boltzmann (corrected by one-dimensional rectangular barrier potential model) sampling with 10000 trajectories.

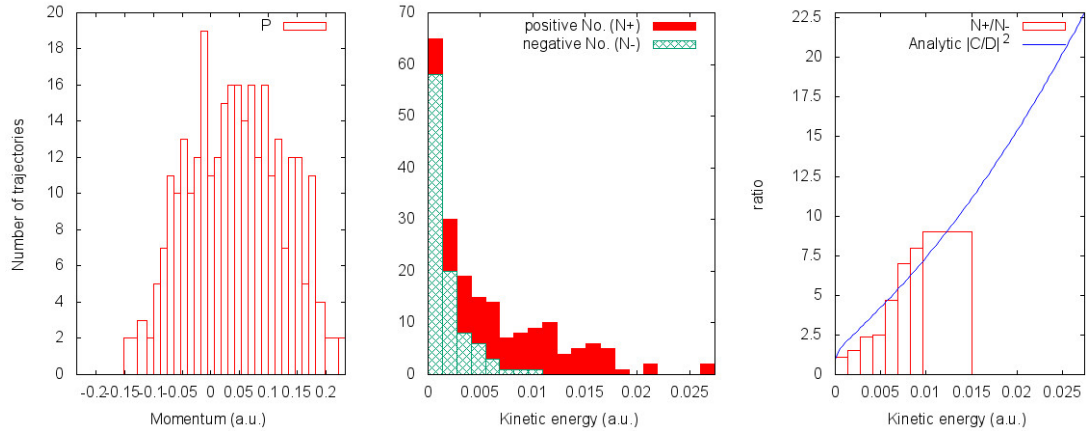


Fig. S5 The distribution of the velocities, the number of positive (N^+) and negative (N^-) trajectories, the ratio $N_+/N_- = |C/D|^2$, respectively along the direction of the reaction path according to corrected Boltzmann sampling with 300 trajectories.

3. Implementation of Global Switching Algorithm in Newton-X.

The simulation process of surface hopping dynamics with global switching algorithm implemented in Newton-X package is showed with the flowchart in Figure S6. In the current implementation of trajectory surface hopping dynamics with Zhu–Nakamura formula for nonadiabatic switching probability, the trajectories are simulated independently using the sampled coordinates and velocities by integration of the Newton equation. The potential energies (total electronic energies) and nuclear gradients are computed on-the-fly by the third-party quantum chemistry programs at each time step. The spin-orbit couplings, if necessary, could be set to constants or be computed on-the-fly also by the third-party programs. To judgement the hopping type (avoided crossing, crossing or parallel in Figure S2 and compute the global switching probability, The potential energies (E_i), nuclear gradients (∇E_i) and spin-orbit couplings (SOC_{ij}) of three consecutive time steps are necessary, and these values are recorded at each time step. Therefore, for the molecular dynamics running at time $t+\Delta t$, the hopping probability is computed for time t using the potential energies (E_i), nuclear gradients (∇E_i) and spin-orbit couplings (SOC_{ij}) at time $t-\Delta t$, t and $t+\Delta t$. If the surface hopping takes place at time t , the dynamics state will be changed, and the nuclear velocities at time t are also adjusted according to self-consistent hopping direction⁷ to maintain the total energy conservation. Then, the new coordinates and velocities at time $t+\Delta t$ will be computed by the coordinates and new velocities at time t . And the potential energies (E_i), nuclear gradients (∇E_i) and spin-orbit couplings (SOC_{ij}) at time $t+\Delta t$ are computed again by the third-party program using the new coordinates. Then the program continues the simulation to the next time step until the simulation reaches the maximum time or terminational condition.

The implementation scheme does not change the basic framework of the original Newton-X pacakge. Therefore, most of the functions including the tools of initial samplings, statistical analyses of trajectories are available for th epresent global switching algorithm after a slight modification.

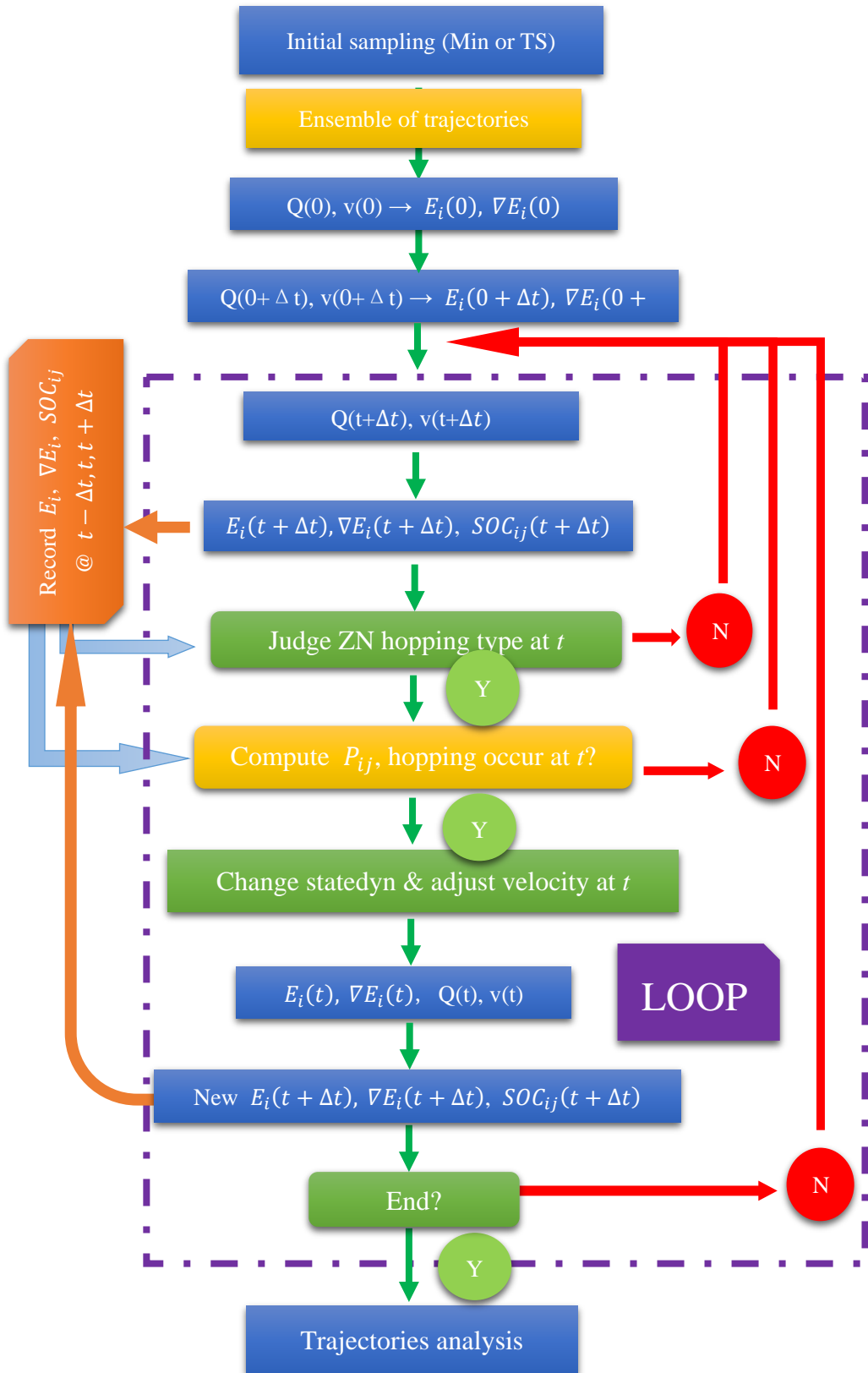


Fig. S6 Flowchart of global switching algorithm implemented in Newton-X package.

4. The Other Figures and Tables.

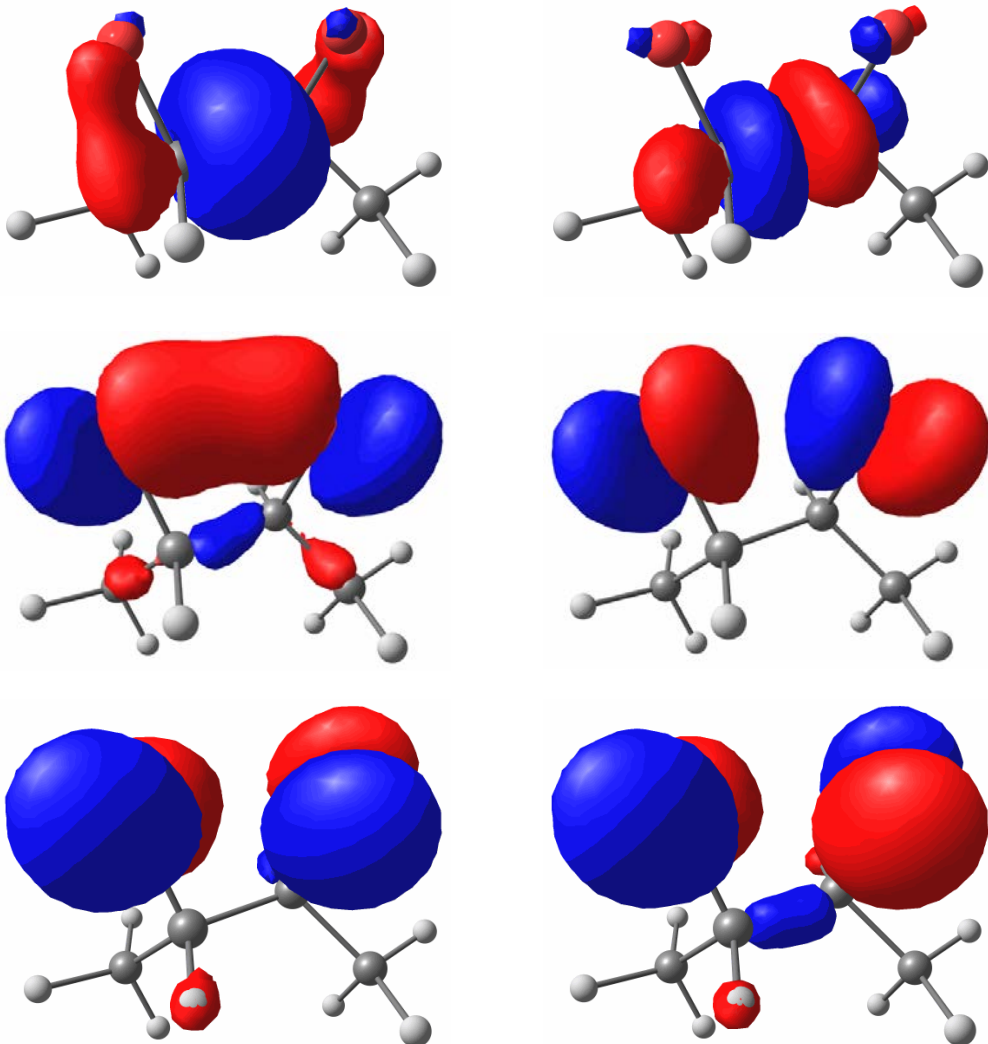


Fig. S7 The active orbitals of 8-in-6 active space used in SA-CASSCF computation.

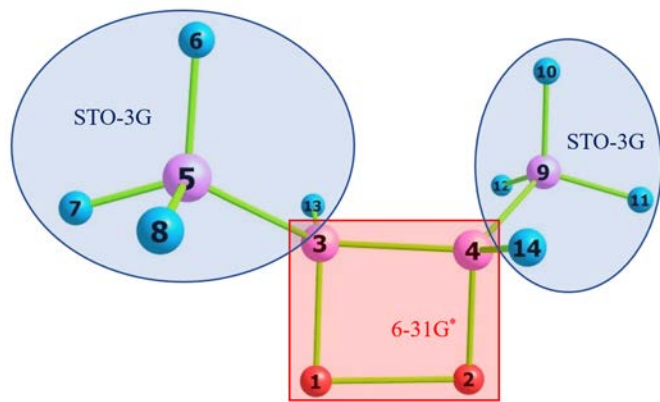


Fig. S8 The labels of atoms and the scheme of the mixing basis sets.

Table S1. The serial number of the internal coordinates (see Figure S8 for the label of atoms).

Internal Number	Type	
1	STRETCHING	C ₃ –C ₄
2	STRETCHING	C ₃ –O ₁
3	STRETCHING	C ₄ –O ₂
4	STRETCHING	C ₃ –C ₅
5	STRETCHING	C ₅ –H ₆
6	STRETCHING	C ₅ –H ₇
7	STRETCHING	C ₅ –H ₈
8	STRETCHING	C ₄ –C ₉
9	STRETCHING	C ₉ –H ₁₀
10	STRETCHING	C ₉ –H ₁₁
11	STRETCHING	C ₉ –H ₁₂
12	STRETCHING	C ₃ –H ₁₃
13	STRETCHING	C ₄ –H ₁₄
14	STRETCHING	O ₁ –O ₂
15	BENDING	O ₁ –C ₃ –C ₄
16	BENDING	O ₂ –C ₄ –C ₃
17	BENDING	C ₅ –C ₃ –C ₄
18	BENDING	H ₆ –C ₅ –C ₃
19	BENDING	H ₇ –C ₅ –H ₆
20	BENDING	H ₈ –C ₅ –H ₆
21	BENDING	C ₉ –C ₄ –C ₃
22	BENDING	H ₁₀ –C ₉ –C ₄
23	BENDING	H ₁₁ –C ₉ –H ₁₀
24	BENDING	H ₁₂ –C ₉ –H ₁₀
25	BENDING	H ₁₃ –C ₃ –C ₅
26	BENDING	H ₁₄ –C ₄ –C ₃
27	TORSION	O ₁ –C ₃ –C ₄ –O ₂
28	TORSION	C ₅ –C ₃ –C ₄ –O ₁
29	TORSION	H ₆ –C ₅ –C ₃ –C ₄
30	TORSION	H ₇ –C ₅ –H ₆ –C ₃
31	TORSION	H ₈ –C ₅ –H ₆ –H ₇
32	TORSION	C ₉ –C ₄ –C ₃ –O ₂
33	TORSION	H ₁₀ –C ₉ –C ₄ –C ₃
34	TORSION	H ₁₁ –C ₉ –H ₁₀ –C ₄
35	TORSION	H ₁₂ –C ₉ –H ₁₀ –C ₄
36	TORSION	H ₁₃ –C ₃ –C ₅ –C ₄
37	TORSION	H ₁₄ –C ₄ –C ₃ –C ₉

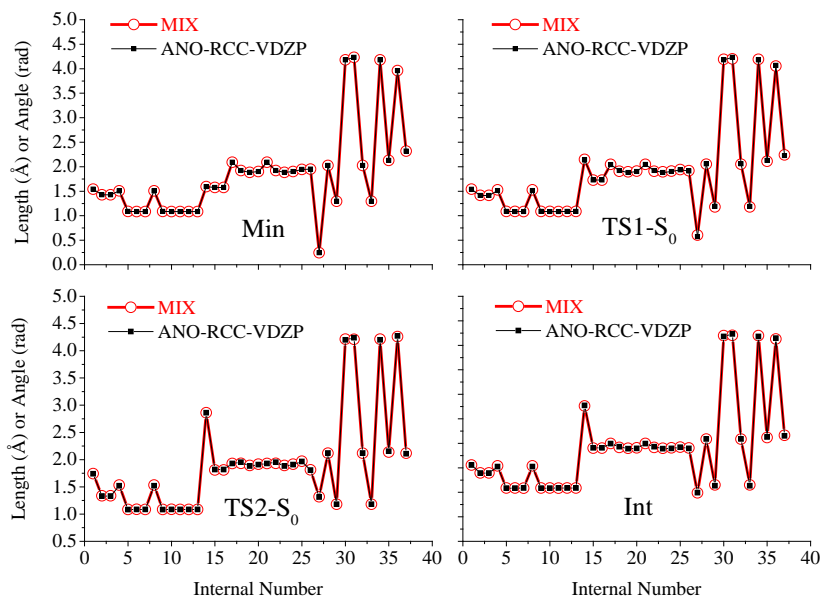


Fig. S9 The comparison of the optimized bond lengths, bond angles and dihedral angles between the mixing and ANO-RCC-VDZP basis sets at SA-CASSCF(8,6) level for stationary points on S₀ surface (Min, TS1-S₀, TS2-S₀ and Int).

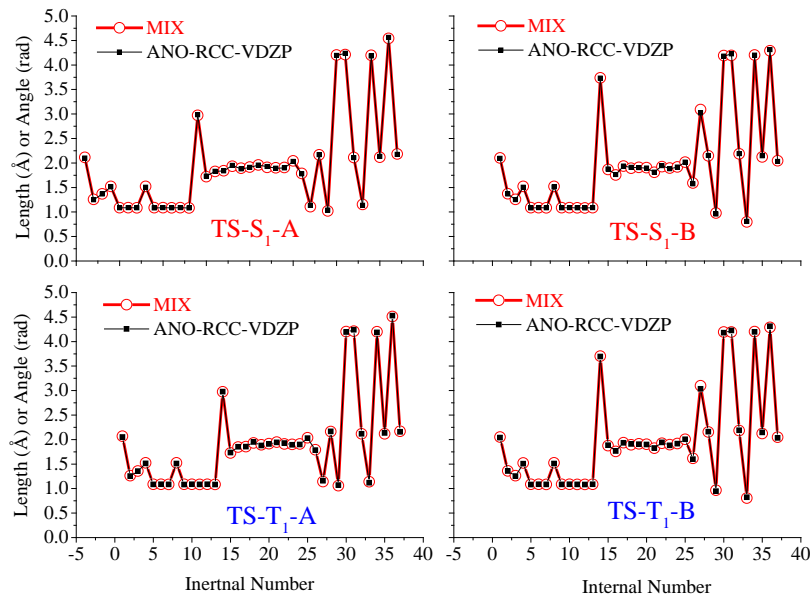


Fig. S10 The comparison of the optimized bond lengths, bond angles and dihedral angles between the mixing and ANO-RCC-VDZP basis sets at SA-CASSCF(8,6) level for stationary points on S₁ (TS-S₁-A and TS-S₁-B) and T₁ (TS-T₁-A and TS-T₁-B) surfaces.

Table S2. The key geometric parameters optimized by SA-CASSCF (normal) and CASPT2 (**bold**) method with 6-31G^{*}+STO-3G mixed basis set (negative paths).

	O ₁ –O ₂	C ₃ –C ₄	O ₁ –C ₃ –C ₄ –O ₂	O ₁ –C ₃ –C ₄ /O ₂ –C ₄ –C ₃	C ₃ –O ₁ /C ₄ –O ₂
Min	1.593	1.542	14.0	90.3/90.3	1.428/1.428
	1.526	1.519	18.3	88.7/88.7	1.466/1.466
TS-S ₀ -	2.154	1.548	-34.9	98.8/98.8	1.419/1.419
	2.300	1.527	-44.0	100.5/100.5	1.426/1.426
Min-S ₁ -70-	2.885	1.568	-68.6	106.9/111.1	1.395/1.390
	2.910	1.534	-66.2	111.2/111.1	1.391/1.396
Min-S ₁ -180	3.583	1.541	170.1	104.9/109.1	1.391/1.435
	3.626	1.539	173.2	109.9/111.4	1.391/1.397
TS-S ₁ -A-	3.256	2.111	-82.7	101.2/108.7	1.257/1.370
	3.134	2.054	-79.4	99.8/108.5	1.262/1.339
TS-S ₁ -B	3.738	2.104	177.1	100.6/107.0	1.258/1.372
	3.67	2.036	176.6	99.5/108.5	1.264/1.341
TS-S ₁ -0	2.560	1.595	-6.0	107.5/122.9	1.387/1.393
	2.618	1.564	3.2	112.2/112.6	1.381/1.383
TS-S ₁ -120-	3.532	1.587	-130.2	112.3/112.3	1.394/1.394
	3.503	1.560	-126.3	113.3/113.3	1.391/1.391
Min-T ₁ -70-	2.930	1.558	-67.3	110.8/110.8	1.394/1.394
	2.902	1.537	-65.1	111.3/111.3	1.390/1.390
Min-T ₁ -180	3.616	1.533	171.7	110.2/110.2	1.397/1.397
	3.626	1.538	172.8	109.9/111.3	1.391/1.401
TS-T ₁ -A-	3.255	2.060	-84.9	101.9/109.7	1.262/1.359
	3.116	1.943	-82.6	101.0/110.0	1.270/1.332
TS-T ₁ -B	3.616	1.533	171.7	110.2/110.2	1.397/1.397
	3.626	1.538	172.8	109.9/111.3	1.391/1.401
TS-T ₁ -0	2.651	1.590	-4.7	112.4/112.4	1.386/1.386
	2.649	1.565	-6.7	112.9/112.9	1.387/1.387
TS-T ₁ -120-	3.531	1.588	-130.5	112.2/112.2	1.393/1.393
	3.534	1.562	-132.9	112.6/112.6	1.392/1.392

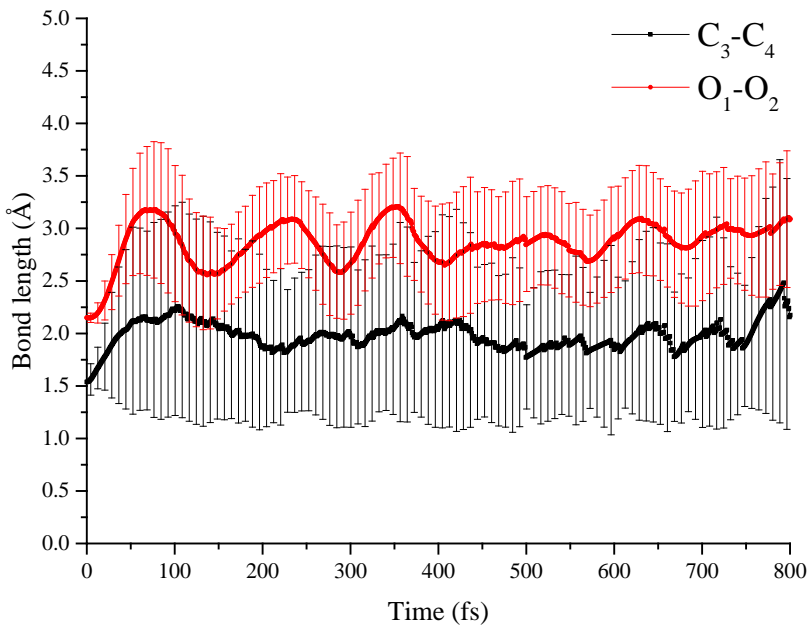


Fig. S11 Time evolution of the ensemble-averaged bond lengths of O_1-O_2 and C_3-C_4 with standard deviations.

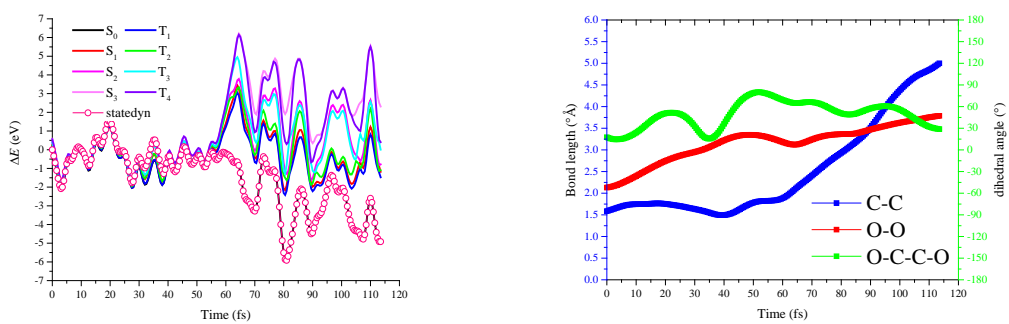


Fig. S12 Time evolution of the potential energies (left) and key geometries (right) of a typical trajectory which ends on the ground S_0 state.

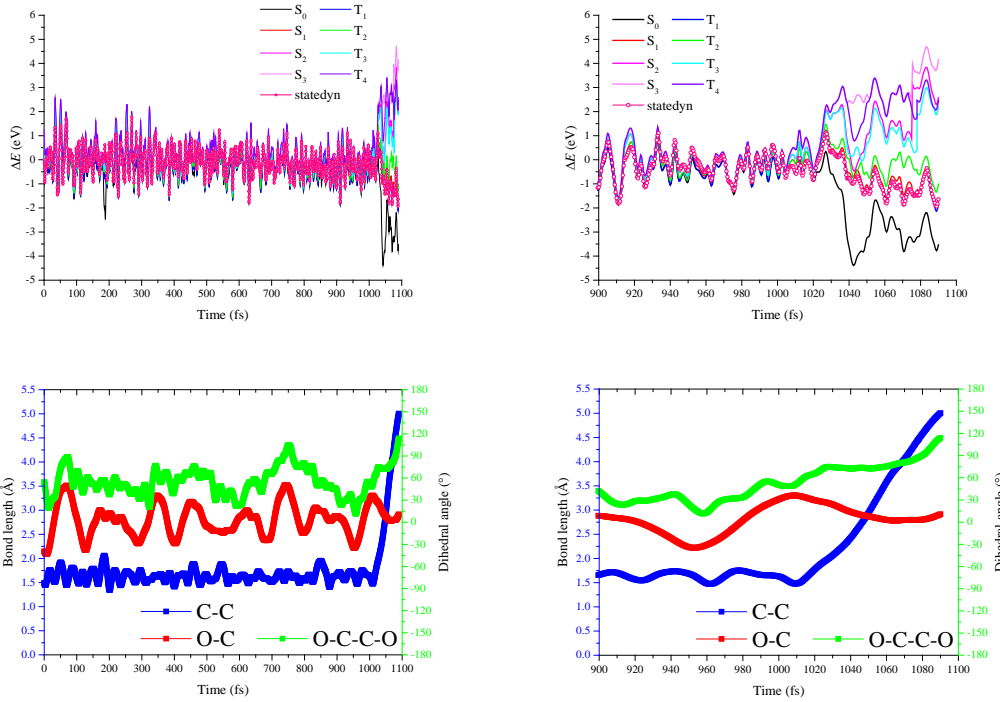


Fig. S13 Time evolution of the potential energies and key geometries of a typical trajectory which ends on the excited S_1 state. The right panels ($400 \sim 575$ fs) are the enlarged graph of the left ones ($0 \sim 600$ fs).

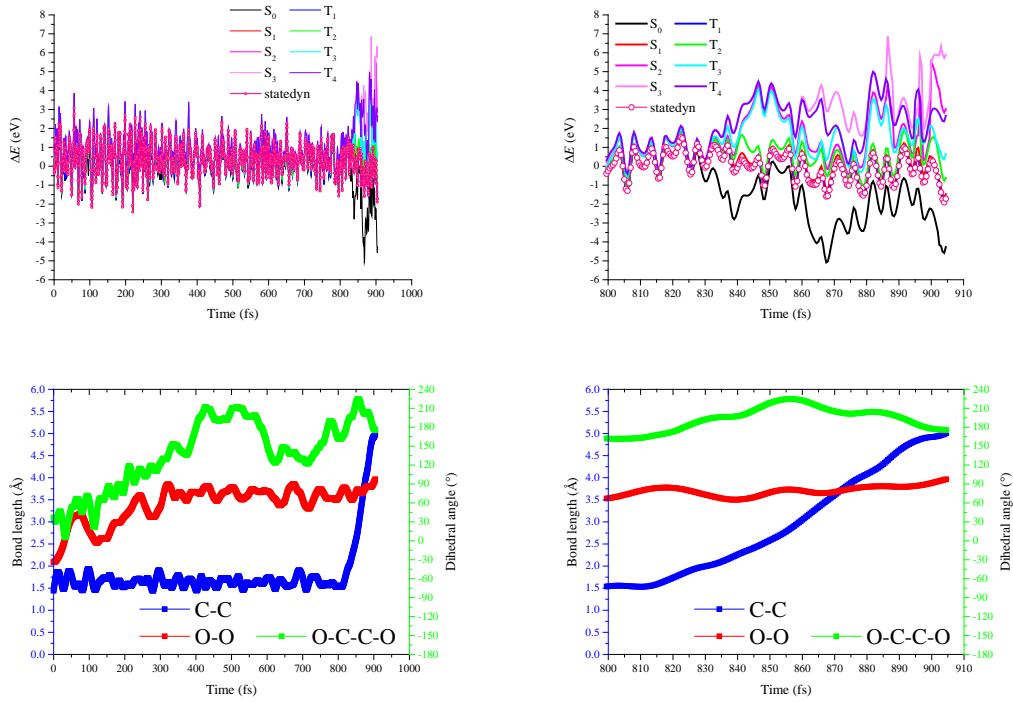


Fig. S14 The same as Figure S13 for typical trajectory which ends on the excited T_1 state. The right panels ($800 \sim 910$ fs) are the enlarged graph of the left ones ($0 \sim 1000$ fs).

5. The Optimized Cartesian Coordinates (\AA) at SA-CASSCF and CASPT2 Levels

Min						
SA-CASSCF			CASPT2			
C	-0.762	-0.922	-0.048	C	-0.753	-0.939
C	0.776	-0.927	0.048	C	0.764	-0.940
O	-0.754	0.496	-0.221	O	-0.704	0.509
O	0.777	0.490	0.224	O	0.719	0.506
C	-1.443	-1.630	-1.190	C	-1.479	-1.671
H	-1.399	-2.706	-1.041	H	-1.447	-2.759
H	-2.488	-1.343	-1.243	H	-2.535	-1.345
H	-0.971	-1.386	-2.135	H	-0.998	-1.455
C	1.452	-1.642	1.189	C	1.489	-1.680
H	1.402	-2.717	1.038	H	1.455	-2.768
H	2.500	-1.361	1.242	H	2.545	-1.357
H	0.982	-1.396	2.135	H	1.009	-1.470
H	-1.225	-1.169	0.903	H	-1.217	-1.121
H	1.237	-1.175	-0.903	H	1.228	-1.117
						-0.932

TS-S ₀						
SA-CASSCF			CASPT2			
C	-0.759	-0.766	-0.076	C	-0.747	-0.726
C	0.774	-0.771	0.077	C	0.762	-0.731
O	-0.934	0.570	-0.511	O	-0.965	0.571
O	0.957	0.563	0.514	O	0.988	0.564
C	-1.366	-1.720	-1.103	C	-1.349	-1.741
H	-1.220	-2.746	-0.772	H	-1.200	-2.759
H	-2.433	-1.533	-1.193	H	-2.432	-1.553
H	-0.894	-1.582	-2.071	H	-0.853	-1.654
C	1.375	-1.730	1.102	C	1.358	-1.752
H	1.222	-2.755	0.769	H	1.203	-2.768
H	2.443	-1.551	1.192	H	2.442	-1.570
H	0.904	-1.592	2.070	H	0.863	-1.663
H	-1.229	-0.885	0.897	H	-1.236	-0.800
H	1.243	-0.891	-0.896	H	1.251	-0.806
						-0.895

TS-S ₀ -						
SA-CASSCF			CASPT2			
C	-0.765	-0.744	-0.053	C	-0.754	-0.773
C	0.780	-0.749	0.054	C	0.769	-0.778
O	-1.006	0.594	0.353	O	-1.045	0.528
O	1.030	0.589	-0.349	O	1.068	0.522
C	-1.309	-1.026	-1.451	C	-1.307	-0.995
H	-1.136	-2.069	-1.709	H	-1.117	-2.040
H	-2.377	-0.829	-1.474	H	-2.394	-0.806
H	-0.812	-0.389	-2.176	H	-0.808	-0.306
C	1.322	-1.037	1.451	C	1.320	-1.006
H	1.142	-2.079	1.707	H	1.124	-2.051
H	2.391	-0.847	1.474	H	2.409	-0.823
H	0.830	-0.398	2.178	H	0.826	-0.315
H	-1.237	-1.381	0.692	H	-1.235	-1.451
H	1.248	-1.387	-0.692	H	1.246	-1.458
						-0.671

Min-T ₁ -70						
SA-CASSCF			CASPT2			
C	-0.763	-0.612	-0.110	C	-0.753	-0.615
C	0.779	-0.617	0.111	C	0.768	-0.618
O	-1.129	0.552	-0.787	O	-1.143	0.545
O	1.152	0.544	0.790	O	1.163	0.536
C	-1.282	-1.791	-0.951	C	-1.285	-1.784
H	-1.128	-2.723	-0.414	H	-1.103	-2.737
H	-2.346	-1.661	-1.130	H	-2.370	-1.653
H	-0.762	-1.836	-1.903	H	-0.767	-1.789
C	1.291	-1.801	0.950	C	1.294	-1.793
H	1.131	-2.731	0.412	H	1.108	-2.744
H	2.355	-1.678	1.129	H	2.380	-1.668
H	0.770	-1.844	1.902	H	0.776	-1.799
H	-1.263	-0.592	0.856	H	-1.256	-0.632
H	1.279	-0.598	-0.855	H	1.271	-0.636
						-0.880

Min-T ₁ -70-			
SA-CASSCF			CASPT2
C	-0.671	-0.802	-0.777
C	0.783	-1.274	-0.476
O	-0.801	-0.419	-2.111
O	1.069	-2.460	-1.152
C	-1.726	-1.878	-0.478
H	-1.672	-2.154	0.572
H	-2.716	-1.489	-0.696
H	-1.539	-2.757	-1.086
C	1.845	-0.232	-0.860
H	1.667	0.685	-0.304
H	2.833	-0.612	-0.618
H	1.787	-0.020	-1.923
H	-0.883	0.093	-0.191
H	0.869	-1.511	0.585
C	-0.656	-0.782	-0.755
C	0.766	-1.276	-0.448
O	-0.785	-0.417	-2.090
O	1.051	-2.450	-1.135
C	-1.726	-1.880	-0.508
H	-1.674	-2.177	0.556
H	-2.729	-1.481	-0.736
H	-1.504	-2.750	-1.150
C	1.851	-0.254	-0.884
H	1.675	0.689	-0.334
H	2.854	-0.646	-0.641
H	1.762	-0.075	-1.969
H	-0.899	0.093	-0.131
H	0.879	-1.470	0.631

Min-T ₁ -180			
SA-CASSCF			CASPT2
C	-0.745	-0.723	-0.146
C	0.767	-0.895	0.041
O	-1.031	0.573	-0.582
O	1.040	-2.121	0.652
C	-1.401	-1.722	-1.114
H	-1.151	-2.733	-0.802
H	-2.479	-1.594	-1.087
H	-1.048	-1.563	-2.128
C	1.602	-0.790	-1.246
H	1.364	0.141	-1.753
H	2.658	-0.811	-0.997
H	1.378	-1.637	-1.924
H	-1.226	-0.815	0.827
H	1.117	-0.139	0.743
C	-0.744	-0.718	-0.169
C	0.767	-0.899	0.056
O	-1.011	0.598	-0.564
O	1.051	-2.147	0.603
C	-1.410	-1.739	-1.113
H	-1.163	-2.758	-0.764
H	-2.503	-1.592	-1.092
H	-1.040	-1.603	-2.143
C	1.610	-0.795	-1.247
H	1.355	0.167	-1.730
H	2.682	-0.813	-0.988
H	1.373	-1.631	-1.925
H	-1.246	-0.777	0.813
H	1.124	-0.123	0.748

TS-T₁-A

SA-CASSCF			CASPT2		
C	-1.108	-0.756	-0.238	C	-1.048
C	0.918	-0.771	0.176	C	0.868
O	-1.158	0.298	-0.930	O	-1.063
O	1.147	0.324	0.949	O	1.056
C	-1.419	-2.095	-0.898	C	-1.388
H	-1.182	-2.917	-0.228	H	-1.209
H	-2.481	-2.133	-1.128	H	-2.460
H	-0.858	-2.201	-1.821	H	-0.792
C	1.338	-2.052	0.889	C	1.314
H	1.198	-2.899	0.223	H	1.165
H	2.390	-1.985	1.158	H	2.389
H	0.748	-2.200	1.788	H	0.727
H	-1.373	-0.657	0.812	H	-1.324
H	1.360	-0.616	-0.801	H	1.282
					-0.599
					-0.825

TS-T₁-A-

SA-CASSCF			CASPT2		
C	-1.121	-0.879	-0.198	C	-1.054
C	0.910	-0.864	0.146	C	0.867
O	-1.522	0.033	0.577	O	-1.435
O	1.500	0.081	-0.632	O	1.426
C	-1.197	-0.680	-1.706	C	-1.165
H	-0.580	-1.414	-2.218	H	-0.570
H	-2.228	-0.805	-2.029	H	-2.228
H	-0.861	0.319	-1.964	H	-0.812
C	1.169	-0.646	1.630	C	1.131
H	0.627	-1.399	2.195	H	0.561
H	2.233	-0.734	1.837	H	2.214
H	0.818	0.337	1.926	H	0.781
H	-1.247	-1.899	0.161	H	-1.174
H	1.188	-1.841	-0.238	H	1.146
					-1.889
					0.200
					-1.806
					-0.292

TS-T ₁ -B						
SA-CASSCF			CASPT2			
C	-0.972	-0.680	-0.028	C	-0.920	-0.679
C	1.081	-0.709	-0.045	C	1.009	-0.702
O	-1.370	-0.676	1.274	O	-1.314	-0.698
O	1.304	-0.765	-1.286	O	1.187	-0.774
C	-1.505	0.515	-0.808	C	-1.458	0.521
H	-1.089	0.484	-1.812	H	-0.996	0.484
H	-2.590	0.463	-0.861	H	-2.558	0.438
H	-1.212	1.443	-0.328	H	-1.186	1.464
C	1.485	0.527	0.749	C	1.446	0.533
H	0.905	0.593	1.665	H	0.882	0.598
H	2.538	0.449	1.009	H	2.523	0.432
H	1.336	1.420	0.152	H	1.291	1.444
H	-1.203	-1.647	-0.459	H	-1.144	-1.648
H	1.120	-1.651	0.497	H	1.068	-1.644
						0.521

Min-S ₁ -70						
SA-CASSCF			CASPT2			
C	-0.761	-0.611	-0.114	C	-0.755	0.007
C	0.777	-0.616	0.115	C	0.760	-0.002
O	-1.114	0.552	-0.800	O	-1.118	1.169
O	1.137	0.543	0.803	O	1.139	1.158
C	-1.286	-1.794	-0.946	C	-1.294	-1.169
H	-1.141	-2.722	-0.399	H	-1.135	-2.115
H	-2.347	-1.657	-1.131	H	-2.375	-1.025
H	-0.761	-1.852	-1.895	H	-0.762	-1.203
C	1.294	-1.804	0.945	C	1.283	-1.182
H	1.144	-2.730	0.396	H	1.111	-2.129
H	2.356	-1.674	1.130	H	2.365	-1.052
H	0.769	-1.860	1.893	H	0.751	-1.205
H	-1.266	-0.577	0.850	H	-1.273	0.018
H	1.282	-0.584	-0.849	H	1.278	-0.004
						-0.864

Min-S ₁ -70-			
SA-CASSCF			CASPT2
C	-0.662	-0.810	-0.782
C	0.785	-1.303	-0.437
O	-0.758	-0.432	-2.116
O	0.976	-2.508	-1.112
C	-1.749	-1.867	-0.521
H	-1.687	-2.191	0.515
H	-2.728	-1.432	-0.703
H	-1.605	-2.724	-1.170
C	1.862	-0.284	-0.819
H	1.710	0.638	-0.262
H	2.844	-0.680	-0.578
H	1.812	-0.076	-1.883
H	-0.859	0.074	-0.178
H	0.804	-1.506	0.634
C	-0.657	-0.782	-0.745
C	0.750	-1.301	-0.421
O	-0.758	-0.402	-2.079
O	1.016	-2.490	-1.101
C	-1.750	-1.865	-0.534
H	-1.712	-2.189	0.521
H	-2.743	-1.440	-0.758
H	-1.542	-2.722	-1.195
C	1.859	-0.303	-0.841
H	1.697	0.643	-0.294
H	2.849	-0.717	-0.583
H	1.792	-0.122	-1.926
H	-0.896	0.086	-0.112
H	0.840	-1.497	0.658

Min-S ₁ -180			
SA-CASSCF			CASPT2
C	-0.762	-0.746	-0.130
C	0.763	-0.874	0.052
O	-0.973	0.614	-0.534
O	1.049	-2.092	0.660
C	-1.392	-1.721	-1.128
H	-1.148	-2.740	-0.839
H	-2.471	-1.603	-1.117
H	-1.027	-1.531	-2.132
C	1.583	-0.814	-1.249
H	1.338	0.105	-1.776
H	2.642	-0.817	-1.006
H	1.358	-1.664	-1.884
H	-1.215	-0.865	0.851
H	1.101	-0.082	0.717
C	-0.744	-0.717	-0.168
C	0.767	-0.900	0.055
O	-1.011	0.595	-0.567
O	1.054	-2.148	0.598
C	-1.412	-1.739	-1.112
H	-1.164	-2.757	-0.761
H	-2.508	-1.592	-1.092
H	-1.042	-1.603	-2.144
C	1.612	-0.792	-1.245
H	1.354	0.168	-1.729
H	2.684	-0.810	-0.984
H	1.377	-1.636	-1.930
H	-1.246	-0.776	0.812
H	1.124	-0.124	0.751

TS-S ₁ .A			
SA-CASSCF			CASPT2
C	-1.136	-0.755	-0.243
C	0.937	-0.789	0.171
O	-1.175	0.307	-0.914
O	1.156	0.331	0.930
C	-1.436	-2.087	-0.919
H	-1.162	-2.916	-0.273
H	-2.504	-2.144	-1.118
H	-0.901	-2.162	-1.860
C	1.356	-2.052	0.912
H	1.219	-2.913	0.265
H	2.406	-1.978	1.185
H	0.762	-2.181	1.812
H	-1.374	-0.674	0.814
H	1.372	-0.646	-0.809
C	-1.101	-0.758	-0.240
C	0.917	-0.769	0.184
O	-1.090	0.312	-0.911
O	1.079	0.333	0.920
C	-1.417	-2.094	-0.907
H	-1.187	-2.937	-0.231
H	-2.500	-2.110	-1.137
H	-0.854	-2.194	-1.849
C	1.344	-2.053	0.904
H	1.190	-2.912	0.226
H	2.417	-1.977	1.165
H	0.749	-2.188	1.825
H	-1.326	-0.685	0.836
H	1.297	-0.625	-0.834

TS-S ₁ -A-			
SA-CASSCF			CASPT2
C	-1.147	-0.886	-0.201
C	0.936	-0.889	0.136
O	-1.518	0.038	0.565
O	1.508	0.087	-0.638
C	-1.211	-0.704	-1.711
H	-0.599	-1.450	-2.211
H	-2.242	-0.824	-2.037
H	-0.865	0.289	-1.978
C	1.202	-0.677	1.618
H	0.684	-1.449	2.182
H	2.269	-0.738	1.817
H	0.827	0.294	1.925
H	-1.263	-1.902	0.173
H	1.216	-1.856	-0.266
C	-1.107	-0.864	-0.176
C	0.927	-0.848	0.103
O	-1.435	0.087	0.586
O	1.450	0.137	-0.638
C	-1.184	-0.726	-1.694
H	-0.606	-1.529	-2.189
H	-2.246	-0.812	-1.991
H	-0.798	0.261	-1.997
C	1.166	-0.688	1.607
H	0.629	-1.502	2.129
H	2.251	-0.753	1.816
H	0.765	0.286	1.936
H	-1.204	-1.892	0.217
H	1.188	-1.822	-0.334

TS-S ₁ -B			
SA-CASSCF			CASPT2
C	-0.990	-0.684	-0.037
C	1.114	-0.713	-0.046
O	-1.385	-0.682	1.278
O	1.338	-0.776	-1.282
C	-1.519	0.517	-0.805
H	-1.109	0.490	-1.811
H	-2.605	0.475	-0.854
H	-1.218	1.441	-0.322
C	1.496	0.529	0.746
H	0.897	0.599	1.651
H	2.543	0.456	1.027
H	1.355	1.417	0.140
H	-1.214	-1.651	-0.468
H	1.126	-1.652	0.503
C	-0.969	-0.682	0.006
C	1.066	-0.702	-0.069
O	-1.348	-0.690	1.293
O	1.228	-0.765	-1.321
C	-1.477	0.520	-0.798
H	-1.000	0.477	-1.794
H	-2.578	0.452	-0.893
H	-1.204	1.461	-0.289
C	1.462	0.533	0.735
H	0.867	0.591	1.665
H	2.532	0.435	1.001
H	1.325	1.442	0.128
H	-1.156	-1.662	-0.450
H	1.081	-1.646	0.503

TS-T ₁ -0			
SA-CASSCF			CASPT2
C	-0.665	-1.002	-1.194
C	0.844	-1.415	-0.913
O	-1.061	-1.292	-2.491
O	1.422	-2.073	-1.988
C	-1.645	-1.623	-0.187
H	-1.356	-1.345	0.825
H	-2.649	-1.259	-0.382
H	-1.631	-2.705	-0.272
C	1.713	-0.222	-0.487
H	1.278	0.254	0.389
H	2.714	-0.567	-0.246
H	1.767	0.505	-1.291
H	-0.746	0.084	-1.152
H	0.860	-2.171	-0.127
C	-0.655	-1.020	-1.206
C	0.836	-1.411	-0.934
O	-1.056	-1.290	-2.506
O	1.419	-2.085	-1.997
C	-1.641	-1.617	-0.177
H	-1.334	-1.314	0.841
H	-2.659	-1.244	-0.383
H	-1.624	-2.718	-0.249
C	1.708	-0.220	-0.477
H	1.253	0.242	0.419
H	2.723	-0.578	-0.234
H	1.759	0.530	-1.285
H	-0.753	0.081	-1.180
H	0.871	-2.188	-0.149

TS-T ₁ -120					
SA-CASSCF			CASPT2		
C	-0.675	-1.369	-1.415	C	-0.662
C	0.902	-1.299	-1.321	C	0.890
O	-1.083	-2.668	-1.722	O	-1.083
O	1.415	-0.545	-2.377	O	1.414
C	-1.469	-0.957	-0.161	C	-1.472
H	-1.234	0.071	0.099	H	-1.221
H	-2.530	-1.032	-0.379	H	-2.548
H	-1.230	-1.603	0.678	H	-1.227
C	1.500	-0.697	-0.036	C	1.503
H	1.179	-1.278	0.824	H	1.165
H	2.583	-0.736	-0.103	H	2.603
H	1.187	0.334	0.091	H	1.184
H	-0.977	-0.739	-2.248	H	-0.980
H	1.278	-2.312	-1.446	H	1.280
					-2.328
					-1.431

TS-T ₁ -120-					
SA-CASSCF			CASPT2		
C	-0.729	-0.718	-0.432	C	-0.714
C	0.790	-1.095	-0.164	C	0.778
O	-0.864	0.259	-1.415	O	-0.851
O	1.003	-2.472	-0.180	O	0.989
C	-1.615	-1.920	-0.796	C	-1.620
H	-1.604	-2.642	0.016	H	-1.611
H	-2.631	-1.571	-0.957	H	-2.647
H	-1.248	-2.402	-1.697	H	-1.242
C	1.780	-0.425	-1.131	C	1.785
H	1.699	0.655	-1.046	H	1.702
H	2.788	-0.735	-0.872	H	2.804
H	1.561	-0.712	-2.155	H	1.557
H	-1.132	-0.239	0.460	H	-1.135
H	1.046	-0.811	0.856	H	1.051
					-0.828
					0.852

TS-S ₁ -0						
SA-CASSCF			CASPT2			
C	-0.651	-0.982	-1.164	C	-0.641	-0.961
C	0.837	-1.449	-0.830	C	0.804	-1.458
O	-1.015	-1.238	-2.478	O	-1.041	-1.338
O	1.325	-2.128	-1.945	O	1.403	-2.107
C	-1.693	-1.638	-0.243	C	-1.694	-1.612
H	-1.455	-1.408	0.793	H	-1.437	-1.334
H	-2.680	-1.250	-0.478	H	-2.703	-1.240
H	-1.682	-2.715	-0.379	H	-1.650	-2.709
C	1.751	-0.271	-0.473	C	1.746	-0.282
H	1.366	0.239	0.407	H	1.392	0.144
H	2.752	-0.633	-0.255	H	2.776	-0.660
H	1.797	0.428	-1.302	H	1.719	0.492
H	-0.703	0.100	-1.059	H	-0.708	0.131
H	0.794	-2.156	-0.004	H	0.779	-2.166
						-0.017

TS-S ₁ -120						
SA-CASSCF			CASPT2			
C	-0.676	-1.362	-1.419	C	-0.666	-1.350
C	0.903	-1.308	-1.319	C	0.894	-1.327
O	-1.089	-2.656	-1.733	O	-1.087	-2.636
O	1.422	-0.560	-2.376	O	1.420	-0.584
C	-1.469	-0.966	-0.159	C	-1.469	-0.980
H	-1.232	0.059	0.113	H	-1.219	0.057
H	-2.530	-1.036	-0.377	H	-2.547	-1.046
H	-1.230	-1.623	0.671	H	-1.219	-1.671
C	1.500	-0.690	-0.040	C	1.500	-0.675
H	1.176	-1.260	0.826	H	1.160	-1.247
H	2.583	-0.732	-0.104	H	2.601	-0.727
H	1.189	0.344	0.072	H	1.180	0.377
H	-0.970	-0.715	-2.242	H	-0.960	-0.659
H	1.269	-2.326	-1.426	H	1.255	-2.363
						-1.386

TS-S₁-120-

SA-CASSCF			CASPT2		
C	-0.729	-0.716	-0.427	C	-0.714
C	0.790	-1.093	-0.159	C	0.772
O	-0.866	0.259	-1.413	O	-0.862
O	1.005	-2.470	-0.179	O	1.003
C	-1.612	-1.918	-0.800	C	-1.607
H	-1.602	-2.643	0.010	H	-1.583
H	-2.629	-1.570	-0.961	H	-2.640
H	-1.242	-2.395	-1.701	H	-1.211
C	1.777	-0.429	-1.132	C	1.773
H	1.698	0.651	-1.052	H	1.679
H	2.786	-0.738	-0.875	H	2.797
H	1.555	-0.720	-2.154	H	1.527
H	-1.135	-0.243	0.467	H	-1.153
H	1.048	-0.803	0.859	H	1.063

6. Detailed internal geometries

Table S3. The optimized bond lengths, bond angles and dihedral angles between the mixing and ANO-RCC-VDZP basis sets at SA-CASSCF(8,6) level for stationary points on S0 surface (Min, TS1-S0)

Internal	Min		TS1-S ₀	
	MIX	ANO-RCC-VDZP	MIX	ANO-RCC-VDZP
1	1.542	1.542	1.541	1.540
2	1.428	1.428	1.416	1.413
3	1.428	1.428	1.416	1.413
4	1.506	1.506	1.528	1.512
5	1.087	1.087	1.088	1.086
6	1.086	1.086	1.087	1.085
7	1.085	1.085	1.085	1.085
8	1.506	1.506	1.528	1.512
9	1.087	1.087	1.088	1.086
10	1.086	1.086	1.087	1.085
11	1.085	1.085	1.085	1.085
12	1.086	1.086	1.087	1.087
13	1.086	1.086	1.087	1.087
14	1.593	1.593	2.150	2.139
15	1.575	1.575	1.727	1.730
16	1.575	1.575	1.727	1.730
17	2.090	2.090	2.049	2.044
18	1.921	1.921	1.908	1.921
19	1.883	1.883	1.896	1.883
20	1.902	1.902	1.909	1.901
21	2.090	2.090	2.049	2.044
22	1.921	1.921	1.908	1.921
23	1.883	1.883	1.896	1.883
24	1.902	1.902	1.909	1.901
25	1.944	1.944	1.941	1.937
26	1.950	1.950	1.918	1.913
27	0.244	0.244	0.604	0.572
28	2.024	2.024	2.052	2.059
29	1.295	1.295	1.180	1.190
30	4.181	4.181	4.193	4.180
31	4.231	4.231	4.201	4.231
32	2.024	2.024	2.052	2.059
33	1.295	1.295	1.180	1.188
34	4.181	4.181	4.193	4.180
35	2.128	2.128	2.111	2.127
36	3.962	3.962	4.053	4.069
37	2.318	2.318	2.241	2.226

Table S4. The optimized bond lengths, bond angles and dihedral angles between the mixing and ANO-RCC-VDZP basis sets at SA-CASSCF(8,6) level for stationary points on S0 surface (TS2-S0, Int).

Internal	TS2-S ₀		Int	
	MIX	ANO-RCC-VDZP	MIX	ANO-RCC-VDZP
1	1.744	1.740	1.555	1.555
2	1.336	1.331	1.396	1.391
3	1.336	1.331	1.396	1.391
4	1.533	1.520	1.538	1.524
5	1.086	1.083	1.086	1.083
6	1.087	1.085	1.086	1.084
7	1.085	1.085	1.086	1.086
8	1.533	1.520	1.538	1.524
9	1.086	1.083	1.086	1.083
10	1.087	1.085	1.086	1.084
11	1.085	1.085	1.086	1.086
12	1.086	1.085	1.088	1.088
13	1.086	1.085	1.088	1.088
14	2.860	2.861	2.763	2.772
15	1.811	1.817	1.901	1.907
16	1.811	1.817	1.901	1.907
17	1.930	1.928	1.998	1.995
18	1.933	1.951	1.917	1.931
19	1.892	1.882	1.900	1.891
20	1.917	1.909	1.907	1.895
21	1.930	1.928	1.998	1.995
22	1.933	1.951	1.917	1.931
23	1.892	1.882	1.900	1.891
24	1.917	1.909	1.907	1.895
25	1.971	1.964	1.923	1.919
26	1.813	1.807	1.906	1.897
27	1.317	1.314	0.990	0.991
28	2.118	2.120	2.085	2.088
29	1.182	1.180	1.152	1.134
30	4.213	4.201	4.198	4.180
31	4.209	4.238	4.202	4.233
32	2.118	2.120	2.085	2.088
33	1.182	1.180	1.152	1.134
34	4.213	4.201	4.198	4.180
35	2.139	2.156	2.116	2.130
36	4.260	4.273	4.128	4.145
37	2.119	2.107	2.165	2.151

7. Spin-orbital coupling matrix elements

Table S5. The absolute value of complex SO-Hamiltonian matrix elements over spin components of spin-free eigenstates of the mixing and ANO-RCC-VDZP basis sets at SA-CASSCF(8,6) level for Min. Print threshold: 5.0 cm⁻¹.

I1	S1	MS1	I2	S2	MS2	MIX	SOC VDZP	Δ
6	1	0	1	0	0	13.667	16.764	3.097
6	1	0	4	0	0	12.613	15.491	2.878
8	1	-1	2	0	0	52.718	64.556	11.838
8	1	-1	6	1	0	48.411	59.3	10.889
9	1	0	1	0	0	11.094	13.951	2.857
9	1	0	3	0	0	10.749	13.098	2.349
9	1	0	5	1	-1	48.411	59.3	10.889
9	1	0	7	1	1	48.411	59.3	10.889
10	1	1	2	0	0	52.718	64.556	11.838
10	1	1	6	1	0	48.411	59.3	10.889
11	1	-1	1	0	0	57.804	70.712	12.908
11	1	-1	4	0	0	47.599	58.31	10.711
11	1	-1	8	1	-1	13.507	16.378	2.871
13	1	1	1	0	0	57.804	70.712	12.908
13	1	1	4	0	0	47.599	58.31	10.711
13	1	1	10	1	1	13.507	16.378	2.871
14	1	-1	2	0	0	51.112	62.583	11.471
14	1	-1	6	1	0	53.653	65.728	12.075
14	1	-1	11	1	-1	12.602	15.382	2.78
15	1	0	3	0	0	14.71	17.926	3.216
15	1	0	5	1	-1	53.653	65.728	12.075
15	1	0	7	1	1	53.653	65.728	12.075
16	1	1	2	0	0	51.112	62.583	11.471
16	1	1	6	1	0	53.653	65.728	12.075
16	1	1	13	1	1	12.602	15.382	2.78

Table S6. The absolute value of complex SO-Hamiltonian matrix elements over spin components of spin-free eigenstates of the mixing and ANO-RCC-VDZP basis sets at SA-CASSCF(8,6) level for TS₁-S₀. Print threshold: 5.0 cm⁻¹.

I1	S1	MS1	I2	S2	MS2	MIX	SOC VDZP	Δ
5	1	-1	1	0	0	6.151	8.091	1.94
5	1	-1	2	0	0	6.591	0.353	-6.238
5	1	-1	4	0	0	6.354	8.366	2.012
6	1	0	1	0	0	25.329	30.136	4.807

6	1	0	4	0	0	27.76	32.611	4.851
7	1	1	1	0	0	6.151	8.091	1.94
7	1	1	2	0	0	6.591	0.353	-6.238
7	1	1	4	0	0	6.354	8.366	2.012
8	1	-1	2	0	0	55.374	68.604	13.23
8	1	-1	3	0	0	5.202	6.858	1.656
8	1	-1	6	1	0	49.427	61.03	11.603
9	1	0	1	0	0	5.534	3.056	-2.478
9	1	0	3	0	0	24.057	28.511	4.454
9	1	0	5	1	-1	49.427	61.03	11.603
9	1	0	7	1	1	49.427	61.03	11.603
10	1	1	2	0	0	55.374	68.604	13.23
10	1	1	3	0	0	5.202	6.858	1.656
10	1	1	6	1	0	49.427	61.03	11.603
11	1	-1	1	0	0	56.207	69.319	13.112
11	1	-1	4	0	0	50.13	61.704	11.574
11	1	-1	8	1	-1	27.473	32.194	4.721
11	1	-1	9	1	0	5.787	7.597	1.81
12	1	0	8	1	-1	5.787	7.597	1.81
12	1	0	10	1	1	5.787	7.597	1.81
13	1	1	1	0	0	56.207	69.319	13.112
13	1	1	4	0	0	50.13	61.704	11.574
13	1	1	9	1	0	5.787	7.597	1.81
13	1	1	10	1	1	27.473	32.194	4.721
14	1	-1	2	0	0	50.177	61.992	11.815
14	1	-1	3	0	0	6.429	8.438	2.009
14	1	-1	6	1	0	55.721	69.036	13.315
14	1	-1	9	1	0	6.495	0.211	-6.284
14	1	-1	11	1	-1	24.899	29.107	4.208
14	1	-1	12	1	0	5.442	7.151	1.709
15	1	0	3	0	0	28.303	32.986	4.683
15	1	0	5	1	-1	55.721	69.036	13.315
15	1	0	7	1	1	55.721	69.036	13.315
15	1	0	8	1	-1	6.495	0.211	-6.284
15	1	0	10	1	1	6.495	0.211	-6.284
15	1	0	11	1	-1	5.442	7.151	1.709
15	1	0	13	1	1	5.442	7.151	1.709
16	1	1	2	0	0	50.177	61.992	11.815
16	1	1	3	0	0	6.429	8.438	2.009
16	1	1	6	1	0	55.721	69.036	13.315
16	1	1	9	1	0	6.495	0.211	-6.284
16	1	1	12	1	0	5.442	7.151	1.709
16	1	1	13	1	1	24.899	29.107	4.208

Table S7. The absolute value of complex SO-Hamiltonian matrix elements over spin components of spin-free eigenstates of the mixing and ANO-RCC-VDZP basis sets at SA-CASSCF(8,6) level for $\text{TS}_2\text{-S}_0$. Print threshold: 5.0 cm⁻¹.

I1	S1	MS1	I2	S2	MS2	MIX	SOC VDZP	Δ
6	1	0	1	0	0	50.686	61.729	11.043
6	1	0	4	0	0	50.196	60.775	10.579
8	1	-1	2	0	0	40.242	49.522	9.28
8	1	-1	3	0	0	5.033	6.454	1.421
8	1	-1	6	1	0	44.033	53.697	9.664
9	1	0	3	0	0	52.522	63.309	10.787
9	1	0	5	1	-1	44.033	53.697	9.664
9	1	0	7	1	1	44.033	53.697	9.664
10	1	1	2	0	0	40.242	49.522	9.28
10	1	1	3	0	0	5.033	6.454	1.421
10	1	1	6	1	0	44.033	53.697	9.664
11	1	-1	1	0	0	42.002	51.365	9.363
11	1	-1	4	0	0	42.408	51.747	9.339
11	1	-1	8	1	-1	47.911	58.901	10.99
13	1	1	1	0	0	42.002	51.365	9.363
13	1	1	4	0	0	42.408	51.747	9.339
13	1	1	10	1	1	47.911	58.901	10.99
14	1	-1	2	0	0	43.982	53.583	9.601
14	1	-1	6	1	0	40.152	49.415	9.263
14	1	-1	11	1	-1	52.592	64.033	11.441
15	1	0	3	0	0	47.945	58.715	10.77
15	1	0	5	1	-1	40.152	49.415	9.263
15	1	0	7	1	1	40.152	49.415	9.263
16	1	1	2	0	0	43.982	53.583	9.601
16	1	1	6	1	0	40.152	49.415	9.263
16	1	1	13	1	1	52.592	64.033	11.441

Table S8. The absolute value of complex SO-Hamiltonian matrix elements over spin components of spin-free eigenstates of the mixing and ANO-RCC-VDZP basis sets at SA-CASSCF(8,6) level for Int. Print threshold: 5.0 cm⁻¹.

I1	S1	MS1	I2	S2	MS2	MIX	SOC VDZP	Δ
5	1	-1	2	0	0	44.595	54.28	9.685
5	1	-1	3	0	0	15.809	19.468	3.659
6	1	0	3	0	0	42.025	51.289	9.264
7	1	1	2	0	0	44.595	54.28	9.685
7	1	1	3	0	0	15.809	19.468	3.659

8	1	-1	1	0	0	15.758	19.63	3.872
8	1	-1	2	0	0	6.469	9.356	2.887
8	1	-1	4	0	0	14.521	17.909	3.388
8	1	-1	6	1	0	47.355	57.94	10.585
9	1	0	1	0	0	42.252	52.155	9.903
9	1	0	4	0	0	38.908	47.594	8.686
9	1	0	5	1	-1	47.355	57.94	10.585
9	1	0	7	1	1	47.355	57.94	10.585
10	1	1	1	0	0	15.758	19.63	3.872
10	1	1	2	0	0	6.469	9.356	2.887
10	1	1	4	0	0	14.521	17.909	3.388
10	1	1	6	1	0	47.355	57.94	10.585
11	1	-1	1	0	0	44.122	53.279	9.157
11	1	-1	4	0	0	48.165	58.676	10.511
11	1	-1	5	1	-1	39.274	48.05	8.776
11	1	-1	6	1	0	14.757	18.231	3.474
11	1	-1	8	1	-1	5.615	8.161	2.546
12	1	0	5	1	-1	14.757	18.231	3.474
12	1	0	7	1	1	14.757	18.231	3.474
13	1	1	1	0	0	44.122	53.279	9.157
13	1	1	4	0	0	48.165	58.676	10.511
13	1	1	6	1	0	14.757	18.231	3.474
13	1	1	7	1	1	39.274	48.05	8.776
13	1	1	10	1	1	5.615	8.161	2.546
14	1	-1	2	0	0	47.356	57.947	10.591
14	1	-1	3	0	0	14.728	18.166	3.438
14	1	-1	6	1	0	6.481	9.371	2.89
14	1	-1	9	1	0	44.594	54.285	9.691
14	1	-1	11	1	-1	41.663	51.263	9.6
14	1	-1	12	1	0	15.69	19.477	3.787
15	1	0	1	0	0	6.061	9.594	3.533
15	1	0	3	0	0	39.197	47.878	8.681
15	1	0	5	1	-1	6.481	9.371	2.89
15	1	0	7	1	1	6.481	9.371	2.89
15	1	0	8	1	-1	44.594	54.285	9.691
15	1	0	10	1	1	44.594	54.285	9.691
15	1	0	11	1	-1	15.69	19.477	3.787
15	1	0	13	1	1	15.69	19.477	3.787
16	1	1	2	0	0	47.356	57.947	10.591
16	1	1	3	0	0	14.728	18.166	3.438
16	1	1	6	1	0	6.481	9.371	2.89
16	1	1	9	1	0	44.594	54.285	9.691
16	1	1	12	1	0	15.69	19.477	3.787
16	1	1	13	1	1	41.663	51.263	9.6

References

1. C. Zhu, *J. Chem. Phys.* 1996, **105**, 4159.
2. C. Zhu, H. Nakamura, *J. Chem. Phys.* 1992, **97**, 8497.
3. C. Zhu, H. Nakamura, *J. Chem. Phys.* 1993, **98**, 6208.
4. L. Yu, C. Xu, Y. Lei, C. Zhu, Z. Wen, *Phys. Chem. Chem. Phys.* 2014, **16**, 25883.
5. M. Merchán, L. Serrano-Andrés, M. A. Robb, L. Blancafort, *J. Am. Chem. Soc.* 2005, **127**, 1820.
6. C. Xu, L. Yu, C. Zhu, J. Yu, Z. Cao, *Sci. Rep.* 2016, **6**, 26768.